THE ASTROPHYSICAL JOURNAL, 508:876–884, 1998 December 1

ACCELERATED AND AMBIENT He ABUNDANCES FROM GAMMA-RAY LINE MEASUREMENTS OF FLARES

GERALD H. SHARE AND RONALD J. MURPHY
E.O. Hulburt Center for Space Research, Naval Research Laboratory, Washington DC 20375; share@osse.nrl.navy.mil
Received 1998 April 22; accepted 1998 July 2

ABSTRACT

The γ-ray lines from ^{7}Be and ^{7}Li produced when flare-accelerated He nuclei interact with ambient He have been found to be surprisingly intense from measurements made by moderate-resolution γ-ray spectrometers on the *Solar Maximum Mission* (*SMM*) and *Compton Gamma Ray Observatory* (*CGRO*) satellites. These high intensities suggest either accelerated α/proton ratios $\gtrsim 0.5$ and/or an He/H abundance greater than 0.1 in the subcoronal regions where the particles interact. We have studied additional γ-ray lines in 20 flares produced by interactions of α particles on ^{56}Fe and other elements to resolve this ambiguity. These measurements indicate, on average, that the ambient He abundance is consistent with accepted photospheric values and that an enhanced concentration of He is present in flare-accelerated particles. Although there is evidence for the presence of accelerated ^{3}He, its concentration is only a fraction of accelerated ^{4}He. These studies also revealed a new weak line in the spectra at $\sim$1.32 MeV that is attributed to an excited state of ^{55}Fe.

Subject headings: solar wind — Sun: abundances — Sun: flares — Sun: photosphere — Sun: X-rays, gamma rays

1. INTRODUCTION

The abundance and isotopic composition of ambient and flare-accelerated helium in the Sun is critical for understanding solar evolution and structure, primordial elemental and isotopic composition, and the acceleration of particles to relativistic energies. Gamma-ray spectroscopy provides an important method for deriving information relating to these studies. The ambient concentration of ^{3}He plays a significant role in the temporal evolution of the 2.223 MeV neutron capture line produced in solar flares. Hua & Lingenfelter (1987) derived a ^{3}He/H ratio of $(2.3 \pm 1.2) \times 10^{-5}$ (90% confidence) for a single flare. Share & Murphy (1997a) suggested that the product of this ratio and the ^{4}He/^{3}He ratio measured in the solar wind provides an independent estimate of the photospheric ^{4}He abundance. They derive an ambient ^{4}He/H ratio ranging from 0.02 to 0.10 for this one flare.

Two nearby γ-ray lines at 0.429 and 0.478 MeV are emitted in the de-excitation of ^{7}Be and ^{7}Li produced when flare-accelerated α particles fuse with ambient ^{4}He. Share & Murphy (1997b) studied these lines in 19 flares observed by the *Solar Maximum Mission* (*SMM*) Gamma Ray Spectrometer (GRS) from 1980 to 1989. The high relative intensities of these lines require that the accelerated α-particle/proton ratio is $\gtrsim 0.5$ if the assumed ambient ^{4}He/H ratio is ~ 0.1. A high flux in the α-^{4}He line was also observed in the 1991 June 4 flare by the Oriented Scintillation Spectrometer Experiment (OSSE) on the *Compton Gamma Ray Observatory* (*CGRO*) (Murphy et al. 1997). Mandzhavidze, Ramaty, & Kozlovsky (1997) performed detailed calculations to confirm the reported excesses and suggested the possibility that the ambient ^{4}He may be enriched in the subcoronal regions where the α particles interact. They also described how γ-ray line spectroscopy can resolve whether the accelerated or ambient ^{4}He is enhanced by comparing intensities of lines at 0.339, 1.00, 1.05, and 1.19 MeV (produced by interactions of α particles on ^{56}Fe) with the intensities of the 0.847 MeV line (produced by proton interactions on ^{56}Fe) and the α-^{4}He fusion lines. They further note that the ^{16}O(^{3}He, p)^{18}F* reaction produces lines at 0.937, 1.040, and 1.080 MeV that complicate the analysis but offer the possibility of measuring accelerated ^{3}He in flares. They suggest that this is possible with high-resolution germanium spectrometers.

We report on spectroscopic studies of data from the moderate-resolution γ-ray spectrometers on *SMM* and *CGRO* to determine whether some constraints can be placed on the accelerated and ambient ^{4}He abundances. As the solar abundance of ^{56}Fe is well known, comparison of the intensities of the α-^{4}He line complex and the α-^{56}Fe lines determines whether a high ambient ^{4}He abundance is responsible for the intense α-^{4}He feature in the *SMM* and *CGRO* spectra. For an ambient ^{4}He/H ratio of 0.1, Mandzhavidze et al. (1997) calculate that the 0.339 MeV line would have only 5% of the strength of the α-^{4}He feature. A higher ^{4}He/H ratio would result in a lower relative line strength. Because the α-^{4}He feature was detected with a significance of at most 7 σ in the *SMM* flares, the presence of the 0.339 MeV line may only be detectable when the spectra of all 19 flares are studied. The α-^{4}He line was detected at a level of 6.3 σ in the 1991 June 4 flare observed by OSSE, so again we expect the 0.339 MeV line to be only marginally detectable if the ambient ^{4}He abundance is 10% or greater. In the following sections we provide evidence that the 0.339 MeV line has been detected, thus suggesting that the ambient ^{4}He abundance, on average, is not significantly greater than about 10% in the interaction region.

Our studies of flare spectra with *SMM* (Murphy et al. 1990; Share & Murphy 1995) revealed the presence of a weak line feature near 1.02 MeV in some flares. Mandzhavidze et al. (1997) compared the intensity of this complex (lines at 1.00, 1.04, 1.05, and 1.08 MeV) with the 0.847 MeV line for the 1981 April 27 flare; they concluded that the data were insufficient to distinguish between the possibilities of high accelerated α/proton (α/p) or high ambient ^{4}He/H as the cause of the observed intense α-^{4}He line features. In this paper we improve our fits to the 1 MeV region of the *SMM* spectra and include fits to all 19 flares.

We also fitted comparable data from the 1991 June 4 flare observed by *CGRO*/OSSE.

In § 2 we describe the fitting procedures for deriving the line intensities relevant to this investigation. These procedures are applied to representative flare spectra and demonstrate the capabilities of resolving these features. The results from fits to the 20 *SMM* and *CGRO* spectra are discussed in § 3. We also perform statistical studies in this section that support the detection of the 0.339 MeV line at a level that would be expected if ^{4}He has a normal abundance in the region where flare-accelerated particles interact. Statistical studies are also performed on lines in the 1 MeV region and suggest the presence of ^{3}He at only a fraction of ^{4}He in the flare-accelerated particles. Our overall conclusions are summarized in § 4.

2. FITS TO FLARE-AVERAGED GAMMA-RAY SPECTRA

We have used spectroscopic data from 19 intense nuclear line flares observed by *SMM*/GRS (Share & Murphy 1995) and from the 1991 June 4 flare observed by *CGRO*/OSSE (Murphy et al. 1997) to estimate the ambient and accelerated He abundances. Both instruments are moderate-resolution spectrometers utilizing NaI crystals. The *SMM*/GRS operates in the range from 0.3 to 8.5 MeV and has 7% energy resolution at 0.662 MeV, and the *CGRO*/OSSE operates in the range from 0.05 to 10 MeV and has a resolution ranging from 7.1% to 9.1%, depending on which of four independent detectors are used (Johnson et al. 1993). We fitted the data in two different spectral ranges, below 0.75 MeV and from 0.3 to 2.5 MeV, in order to optimize the detection of individual line features.

2.1. *Spectral Fits for* 0.339 MeV *Line*

The 0.339 MeV and α-^{4}He fusion-line fluxes were obtained by fitting the 19 *SMM*/GRS spectra between 0.3 and 0.75 MeV and the *CGRO*/OSSE spectrum of the 1991 June 4 flare between 0.24 and 0.75 MeV. This is the same energy range used previously to obtain measurements of the α-^{4}He fusion lines alone (Share & Murphy 1997b). We used an incident photon model containing a bremsstrahlung function, a narrow 0.339 MeV line, the blended fusion lines for an assumed isotropic distribution of particles (Murphy, Kozlovsky, & Ramaty 1988), a narrow 0.511 MeV annihilation line, a positronium continuum, and instrumentally degraded radiation from higher energy nuclear lines. We used a simple power-law in energy to represent the bremsstrahlung continuum and obtained its amplitude and index. For this study we have fixed the 0.511 MeV annihilation line energy and set its width at a nominal 0.010 MeV; the amplitude of the line is a free parameter. The amplitude of the positronium continuum is also a free parameter but is constrained to be positive. The amplitude of the degraded nuclear component reflects the nuclear de-excitation and 2.223 MeV line fluxes. The composite model, with initial estimates of the free parameters, is folded through a matrix representing the instrument response function and compared with the observed count spectrum. The values of the parameters are then sequentially varied using a computer algorithm until the χ^2 parameter is minimized. The fits were performed separately on spectra from each of the 19 flares observed by *SMM*/GRS and on spectra from each of the four OSSE detectors. Representative spectra and fits from the two instruments are shown in Figure 1.

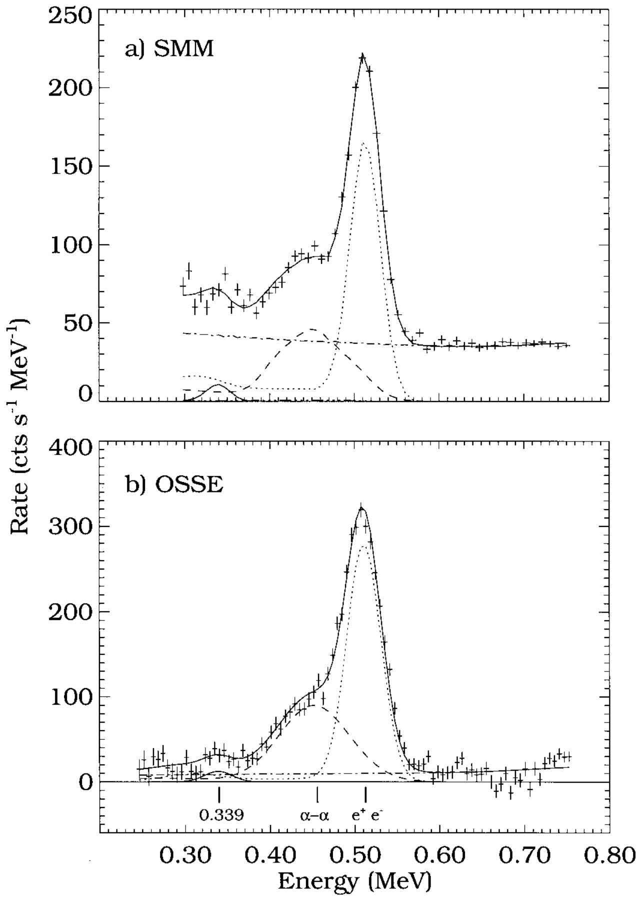

FIG. 1.—(*a*) Summed spectrum from five strong flares observed by the *SMM*/GRS after subtracting the intense bremsstrahlung component. (*b*) Summed spectrum from four *CGRO*/OSSE detectors during the latter portion of 1991 June 4 flare after subtracting the intense bremsstrahlung component. Curves show fits to the data. *Solid line:* overall model (and line at 0.339 MeV from α-^{56}Fe interactions). *Dotted line:* 511 keV line (and positronium continuum for OSSE). *Dashed line:* α-^{4}He fusion line. *Dot-dashed line:* instrument degraded radiation from higher energy nuclear lines. *Dash–double-dotted line:* positronium continuum barely detected by *SMM*.

In Figure 1*a* we plot the summed spectrum from five *SMM*/GRS flares that produced α-^{4}He line fluences greater than 15 γ cm^{-2} and that were well fitted (>15% probability) by the model spectrum. The five flares occurred on 1981 April 27, 1988 December 16, 1989 March 10, August 16, and October 24; the individual spectra are plotted in Share & Murphy (1997b). The best-fitting power-law component has been subtracted in order to reveal the line features of interest. There is only weak evidence for a positronium continuum in these flares; this is related to the high temperature and density in the region where the particles interact (Share, Murphy, & Skibo 1996). It is also of interest to note that the γ-ray spectral shape for an isotropic α-particle distribution used to fit the fusion lines appears to extend to lower energies than the data. We have determined that this is not due to problems with excess broadening in the instrumental response. We can obtain improved fits if we use a fan beam distribution calculated for heliocentric angles less than 35°; however, only one of the five flares occurred at such a small angle. Whether this difference may have a physical origin, such as relativistic beaming leading to loss of redshifted photons, requires further study of the data from these flares and additional flares observed by OSSE.

The best fit indicates the presence of a weak line feature near 0.339 MeV to account for excess counts near that energy. Unfortunately this conclusion is affected by the residual channel-to-channel systematic variations in the summed spectrum below 0.4 MeV; these variations are attributed to the large numbers of counts from the steep bremsstrahlung continuum that, after subtraction, reveals differential nonlinearities in the pulse-height analyzer.

In Figure 1*b* we plot the summed spectrum of the 1991 June 4 flare observed by the four *CGRO*/OSSE detectors. The data were accumulated for 1250 s late in the flare when instrumental saturation effects were minimal. The intense bremsstrahlung continuum has again been subtracted. Both the 0.511 MeV annihilation and α-^{4}He lines are clearly evident, as in the *SMM* spectrum. A Gaussian has been used to fit the OSSE α-^{4}He feature (in a future study we plan to fit these data with the models reflecting different α-particle directional distributions, as done with the *SMM*/GRS). The α-^{4}He line fluence relative to the sum of fluences from high–first ionization potential (FIP) line elements in this flare is about 3 σ above the average value measured by the *SMM*/GRS. The degraded nuclear component is significantly lower in the *CGRO*/OSSE spectrum than in *SMM*/GRS because the larger OSSE shield is more effective at reducing the partial energy losses in the central NaI detector. The spectrum also exhibits evidence for a weak line feature near 0.339 MeV, although there once again appear to be systematic variations that weaken the requirement for such a line.

At this stage of the analysis it is interesting to estimate the mean ratio of fluxes observed in the 0.339 MeV and α-^{4}He complexes for the five-flare sum *SMM* and the *CGRO* spectra. Because of the systematic effects due to high count rates that produced relatively poor fits (reduced χ^2 of $\sim$1.5 to 2), we have added a systematic uncertainty to the errors. We obtain 0.339 MeV/α-^{4}He line ratios of 0.08 ± 0.04 and 0.06 ± 0.03 for *SMM*/GRS and *CGRO*/OSSE, respectively. These are close to the predicted value of $\sim$0.05 calculated by Mandzhavidze et al. (1997) for 10% ambient ^{4}He abundance. Note that the ratio is spectral dependent and has been calculated for an accelerated-particle power-law index of 4. The deduced 1991 June 4 flare particle spectrum is consistent with this index. For an assumed α/p ratio of 0.1, the indices of four of the five *SMM* flares are within 1 σ of 4 and their mean is 3.96; for an α/p ratio of 0.5, indices of three of the five flares are within 1 σ of 4 and their mean is 4.4. Studies of the 0.339 MeV/α-^{4}He ratios in individual flares are presented below. Thus there is evidence from the *SMM* and OSSE data that the ambient ^{4}He abundance is consistent with the accepted photospheric abundance (^{4}He/H $\sim$ 8%).

2.2. *Spectral Fits for* $\sim$1 MeV *Lines*

We fitted the 19 *SMM*/GRS flare spectra and the 1991 June 4 OSSE spectrum over the range from $\sim$0.3 to 2.5 MeV to obtain information on the complex of lines between 0.9 and 1.2 MeV produced by both accelerated ^{4}He interactions on ^{56}Fe and ^{3}He interactions on O. This broad energy range for the fits was necessary in order to properly constrain the electron bremsstrahlung component. In addition to this single power law, the incident photon model contained the following: narrow Gaussian lines at 0.511, 0.847, 0.937, 1.19, 1.238, 1.317, 1.369, 1.634, 1.778, and 2.223 MeV, significantly broadened features at 0.454, 0.811, 1.515, and 1.673 MeV (Murphy et al. 1990), and a template representing the degraded radiation from de-excitation lines of C and O above 2.5 MeV. We used two templates to fit the composite feature near 1.02 MeV based on the calculated spectra shown in Figure 3 of Mandzhavidze et al. (1997) for ^{3}He/^{4}He = 0 and 1 ($\alpha/p = 0.1$; the shape is similar for $\alpha/p = 0.5$). The 1.317 MeV line appears to be necessary to explain broadening observed in the summed spectrum below the strong ^{24}Mg line at 1.369 MeV. This line appears in the calculated solar γ-ray line spectrum presented in Ramaty & Lingenfelter (1995) and comes from the excited state of ^{55}Fe produced in (p, pn) spallation reactions.

Figure 2 displays the results of passing this photon model through the *SMM*/GRS instrument response function and fitting the summed spectrum of the 19 strong nuclear line flares. We display the fits only over the 0.7–1.5 MeV range that contains the lines relevant to this paper. Over this range the fits are excellent and yield a reduced χ^2 of 1.0. In

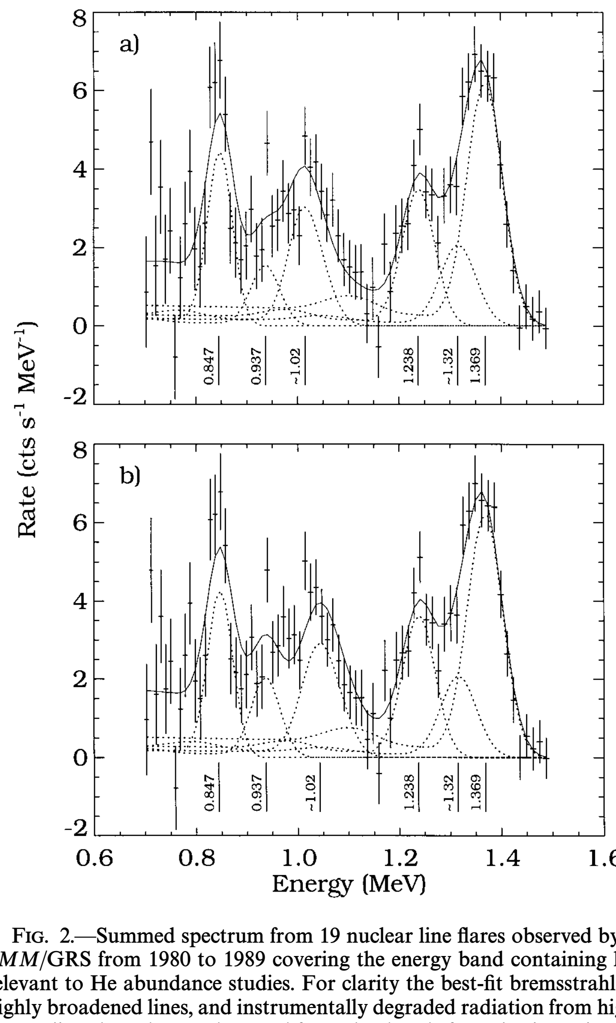

FIG. 2.—Summed spectrum from 19 nuclear line flares observed by the *SMM*/GRS from 1980 to 1989 covering the energy band containing lines relevant to He abundance studies. For clarity the best-fit bremsstrahlung, highly broadened lines, and instrumentally degraded radiation from higher energy lines have been subtracted from the data before plotting. Fits were performed from 0.3 to 2.5 MeV. The overall fit is shown by the solid curve and fits to the individual line features are shown by the dotted curves. The spectra have been calculated for flare-accelerated particles having $\alpha/p = 0.1$ and (*a*) ^{3}He/^{4}He = 0 and (*b*) ^{3}He/^{4}He = 1. The composite feature at $\sim$1.02 MeV is made up of lines at 1.00 and 1.05 MeV from α-^{56}Fe interactions and at 1.04 and 1.08 MeV from ^{3}He-^{16}O interactions. Other line origins: p-^{56}Fe, 0.847 and 1.238 MeV; ^{3}He-^{16}O, 0.937 MeV; p-^{55}Fe, 1.317 MeV; and p-^{24}Mg, 1.369 MeV.

TABLE 1

AVERAGE LINE FLUXES FROM 19 *SMM*/GRS FLARES

ENERGY OF LINE FEATURE (MeV)	FLUX IN FEATURE (10^{-3} γ cm^{-2} s^{-1})	
	$^3He/^4He = 0$	$^3He/^4He = 1$
0.847	2.13 ± 0.30	2.04 ± 0.32
0.937	0.92 ± 0.26	1.21 ± 0.27
~1.02	2.24 ± 0.29	2.41 ± 0.31
1.238	2.74 ± 0.32	2.85 ± 0.32
1.317	1.85 ± 0.37	1.86 ± 0.37
1.369	5.68 ± 0.37	5.68 ± 0.37

this representation we have subtracted the power law, all the broad lines, and higher energy components that yield counts in the energy band before plotting. This leaves only the contributions from narrow lines at 0.847, 0.937, 1.19, 1.238, 1.317, and 1.369 MeV, and the ~1.02 MeV complex, which are all shown by dotted lines. In Figure 2*a* we plot the fit for an incident spectrum produced by accelerated particles with no ^3He, and in Figure 2*b* we plot the fit for particles having a $^3He/^4He$ ratio of 1. The fit is only slightly better ($<1\ \sigma$ significance) for $^3He/^4He = 0$; in this case the model appears to be shifted to lower energies than the data. In contrast, the $^3He/^4He = 1$ model appears to be shifted to higher energies than the data. This suggests an intermediate value for the $^3He/^4He$; however, as Mandzhavidze et al. (1997) point out, the partial cross sections for the ^3He lines are not well known and this can affect the line shape used in fitting the data.

Lines at 0.847, ~1.02, 1.24, and 1.36 MeV are clearly required. The fits over the displayed energy range are excellent (χ^2/degrees of freedom = 1.03) for both cases. The line at 0.847 MeV from proton interactions on ^{56}Fe appears to be somewhat narrower than one would expect from the instrument response at that energy (6.5% FWHM); we attribute this to statistics because no Doppler broadening was assumed for the incoming line photons and there is no reason to assume that the instrumental resolution has changed since launch. Listed in Table 1 are the derived line fluxes from this composite of 19 flares. The intensities for the two ^3He assumptions are not significantly different. There is a suggestion for an increase in the fluence in the ~1.02 MeV complex for the $^3He/^4He = 1$ model that is consistent with the presence of some ^3He in the accelerated particles. Since the ~1.02 MeV/0.847 MeV line ratio is dependent on the spectral index of the accelerated particles, it is not appropriate to compare this flare-averaged ratio with the calculations of Mandzhavidze et al. (1997) for an index of 4. These comparisons are best done on a flare-by-flare basis as discussed below.

3. RESULTS OF FITS TO INDIVIDUAL FLARE SPECTRA

The 19 *SMM*/GRS and the *CGRO*/OSSE 1991 June 4 flare spectra were individually fitted using the models described in §§ 2.1 and 2.2 and illustrated in Figures 1 and 2. Derived line fluences for features relevant to our study of ambient and accelerated He abundances are listed in Table 2. These include the 0.339 MeV, α-^{4}He, 0.847 MeV, 0.937 MeV, ~1.02 MeV lines and the sum of lines at 0.847, 1.238, 1.369, and 1.778 MeV primarily arising from elements with low first ionization potential (FIP). We use this summed low-FIP fluence in our later analyses as a substitute for the 0.847 MeV line fluence in order to improve statistics. Two entries are given for the ~1.02 MeV feature: one for a line profile calculated for an accelerated-particle composition with $^3He/^4He = 0$ and one for $^3He/^4He = 1$ (we used an α/p ratio = 0.1; the results are not significantly different for $\alpha/p = 0.5$).

3.1. *Comparison of* 0.339 MeV *and* α-^{4}He *Lines*

In Figure 3 we plot a comparison of fluences observed in the 0.339 MeV line produced in α-particle interactions on ambient ^{56}Fe with those from the α-^{4}He fusion lines for the 20 flares. The uncertainties reflect the quality of fits and channel-to-channel systematic variations at low energies. The line shows the best fit assuming that the 0.339 MeV and

TABLE 2

MEASURED LINE FLUENCES

NUMBER	DATE	FLUENCE (γ cm^{-2})						
						~1.02 MeV Feature		
		0.339 MeV	α-α	0.847 MeV	0.937 MeV	$^3He/^4He = 0$	$^3He/^4He = 1$	Low FIP
1	1981 Apr 10	1.7 ± 2.3	7.7 ± 6.4	2.1 ± 1.1	0.4 ± 1.0	0.6 ± 1.0	1.4 ± 1.1	10.4 ± 2.4
2	1981 Apr 27	7.9 ± 4.4	44.7 ± 12.2	4.3 ± 2.4	0.8 ± 2.0	6.4 ± 2.2	5.1 ± 2.4	33.3 ± 5.2
3	1982 Jun 3	−1.9 ± 3.7	−8.4 ± 10.7	1.4 ± 2.3	−1.3 ± 2.1	−0.8 ± 2.3	−0.2 ± 2.4	9.4 ± 5.1
4	1982 Jul 9	−1.6 ± 3.8	19.6 ± 9.8	2.2 ± 1.4	0.4 ± 1.1	2.1 ± 1.2	2.8 ± 1.3	16.8 ± 2.6
5	1982 Nov 6	3.9 ± 2.2	11.0 ± 5.8	3.0 ± 1.1	1.4 ± 0.9	0.8 ± 1.0	1.2 ± 1.0	6.7 ± 2.2
6	1982 Dec 7	10.5 ± 12.0	−4.6 ± 31.2	−1.0 ± 3.2	3.2 ± 2.7	4.5 ± 2.8	8.7 ± 3.0	43.5 ± 6.2
7	1984 Apr 24	−0.3 ± 4.1	−8.0 ± 11.9	4.1 ± 1.9	0.5 ± 1.7	−1.3 ± 1.8	−2.9 ± 2.0	23.3 ± 4.3
8	1986 Feb 6	1.8 ± 2.7	2.2 ± 7.1	2.0 ± 1.8	1.0 ± 1.5	6.1 ± 1.6	6.8 ± 1.8	12.2 ± 3.7
9	1988 Dec 16	13.2 ± 7.8	106.4 ± 19.8	8.9 ± 3.3	6.3 ± 2.8	3.5 ± 3.0	3.4 ± 3.3	40.9 ± 6.9
10	1989 Mar 6	37.7 ± 14.8	116.9 ± 38.6	18.4 ± 3.8	0.1 ± 3.1	4.0 ± 3.3	0.2 ± 3.5	101.1 ± 7.4
11	1989 Mar 10	14.6 ± 6.5	42.1 ± 17.6	6.8 ± 2.9	4.0 ± 2.4	8.2 ± 2.6	6.4 ± 2.8	34.9 ± 5.9
12	1989 Mar 17	−2.1 ± 3.8	11.9 ± 9.8	−0.2 ± 1.7	2.3 ± 1.4	5.4 ± 1.5	8.2 ± 1.6	11.8 ± 3.4
13	1989 May 3	−2.3 ± 2.5	11.0 ± 6.9	1.9 ± 1.6	1.6 ± 1.4	2.1 ± 1.5	1.4 ± 1.6	5.0 ± 3.5
14	1989 Aug 16	1.1 ± 2.3	24.5 ± 6.5	3.2 ± 1.4	1.8 ± 1.2	2.5 ± 1.3	1.8 ± 1.4	14.0 ± 3.0
15	1989 Aug 17	5.4 ± 5.7	18.7 ± 15.8	2.2 ± 3.0	2.9 ± 2.5	3.4 ± 2.6	4.4 ± 2.8	10.6 ± 5.7
16	1989 Sep 9	−1.9 ± 2.0	3.5 ± 5.2	0.5 ± 1.1	−1.0 ± 1.0	−0.6 ± 1.0	−0.4 ± 1.1	7.1 ± 2.4
17	1989 Oct 19	3.1 ± 5.2	84.1 ± 14.5	5.0 ± 2.8	0.9 ± 2.4	3.4 ± 2.6	0.4 ± 2.9	41.3 ± 6.1
18	1989 Oct 24	9.8 ± 4.3	17.8 ± 10.8	−0.9 ± 1.5	4.1 ± 1.2	3.2 ± 1.3	4.5 ± 1.4	9.4 ± 2.9
19	1989 Nov 15	−1.1 ± 3.6	13.9 ± 9.5	0.2 ± 1.6	0.0 ± 1.3	2.5 ± 1.4	4.3 ± 1.6	7.0 ± 3.3
20	1991 Jun 4	1.3 ± 0.8	26.1 ± 2.7	1.6 ± 1.3	1.3 ± 1.1	4.5 ± 1.1	4.8 ± 1.1	18.3 ± 2.5

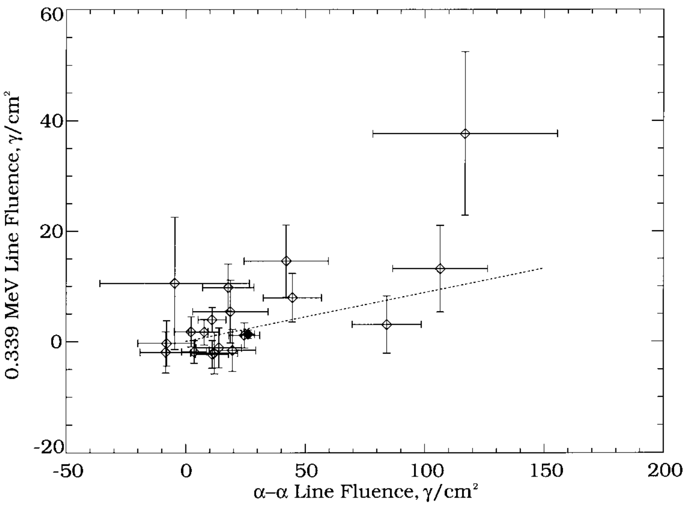

FIG. 3.—Comparison of 0.339 MeV line fluences (produced by α-particle interactions on ^{56}Fe) with fluences in the ^{7}Li and ^{7}Be lines (produced by α-particle reactions on ^{4}He). Filled symbol is the OSSE observation of the 1991 June 4 flare. The dashed line shows the best-fitting slope, 0.088 ± 0.025.

α-^{4}He lines are correlated; the slope is 0.088 ± 0.025. The flare on 1989 February 6 produced the highest nuclear line yield, including the α-^{4}He line; our fits also reveal a high fluence in the 0.339 MeV line for this flare. There is some concern about this point because the spectra had rather large channel-to-channel variations between 0.3 and 0.4 MeV that produced an unacceptably high χ^2; for this reason it was not included in the summed spectrum shown in Figure 1. Even excluding this point there still is evidence for a correlation between the 0.339 MeV and the α-^{4}He *fluences*; the best-fit slope is 0.078 ± 0.25. Such a correlation is not evident when we compare the *fluxes* observed in these lines. Had the correlation been due to a systematic in the fitting procedure, we would have expected any correlation to be stronger in the comparison of *fluxes* because this is more sensitive to background features independent of flare duration. These arguments suggest that the 0.339 MeV line detected here may indeed be of solar origin.

Estimation of the 0.339 MeV/α-^{4}He line ratio in flares is important for determining the ambient ^{4}He abundance in the interaction region. However, taking weighted means of the individual flare line ratios does not yield the correct mean when uncertainties are large and some ratios are close to 0, as is the case here. Instead, we obtain the flare-averaged 0.339 MeV/α-^{4}He ratio using χ^2 as the relevant statistical parameter. In this procedure we determine the constant that when multiplied by the α-^{4}He line fluences produces a minimum χ^2 when compared with the observed 0.339 MeV line fluences. This constant is thus the best-fitting average ratio. The 1 σ uncertainties on the ratio were determined using the values derived for $\Delta\chi^2 = 1$. We performed this procedure for three samples of flares: (1) all 20 flares, and only those flares with accelerated-particle spectral indices within 1 σ of 4 determined under the assumption that the accelerated α/p ratio is either (2) 0.1 or (3) 0.5. We performed the latter two tests because the calculated 0.339 MeV/α-^{4}He ratio has been published by Mandzhavidze et al. (1997) only for a spectral index of 4. Although the weighted means of the derived spectral indices for all 20 flares are 3.9 and 4.4, for α/p of 0.1 and 0.5, there is a large spread in the individually determined indices. As the line ratio is likely to have a dependence on spectral variation it is most reliable to limit the samples based on spectral index.

We derived the following 0.339 MeV/α-^{4}He line ratios using this χ^2 analysis for the three samples: (1) all flares, 0.088 ± 0.024; (2) only flares with index ≅4 assuming $\alpha/p = 0.1$, 0.075 ± 0.025, or (3) only flares with index ≅4 assuming $\alpha/p = 0.5$, 0.10 ± 0.04. The expected ratios determined from calculated spectra plotted in Mandzhavidze et al. (1997) are 0.053 and 0.059 for α/p of 0.1 and 0.5, respectively. Table 3 compares the mean observed/calculated 0.339 MeV line ratios. These ratios were calculated for an assumed ambient ^{4}He/H ratio of 0.10. Thus the *SMM* and OSSE flare observations suggest ambient ^{4}He/H abundance ratios ranging (±1 σ) from 0.053 to 0.106 ($\alpha/p = 0.1$) and from 0.042 to 0.098 ($\alpha/p = 0.5$). On average, the derived helium abundance in the interaction region is consistent with accepted photospheric abundances (^{4}He/H ∼ 0.08). Owing to the weakness of the line feature, however, we cannot rule out significantly higher ^{4}He/H ratios. For example flare-averaged ^{4}He/H ratios up to 0.20 ($\alpha/p = 0.1$) and 0.31 ($\alpha/p = 0.5$) are still acceptable at the 5% confidence level for the limited number of flares having spectral indices consistent with 4.

3.2. *Comparison of Lines Near* 1 MeV

Comparison of the strength of the ∼1.02 MeV line complex with that of the ^{56}Fe line at 0.847 MeV is another key element in determining the helium abundance in flares. Mandzhavidze et al. (1997) have calculated the spectral dependence of the ∼1.02/0.847 line ratio for assumed α/p ratios of 0.1 and 0.5. Forming such ratios for all the flares

TABLE 3

COMPARISON OF MODELS

	MEAN OBSERVED/CALCULATED LINE RATIO[a]		
MODEL	0.339 MeV[b]	0.937 MeV[c]	∼1.02 MeV[d]
$\alpha/p = 0.1$			
Model a $^{3}He/^{4}He = 0$	1.4 ± 0.5	3.2 ± 1.3	3.1 ± 0.5
Model b $^{3}He/^{4}He = 1$	...	0.35 ± 0.11	0.92 ± 0.17
$\alpha/p = 0.5$			
Model c $^{3}He/^{4}He = 0$	1.7 ± 0.7	4.6 ± 1.8	1.33 ± 0.21
Model d $^{3}He/^{4}He = 1$	...	0.10 ± 0.04	0.15 ± 0.04

[a] For ambient ^{4}He/H = 0.1.
[b] Independent of $^{3}He/^{4}He$; spectral indices consistent with 4.
[c] Only flares with spectral indices consistent with 4.
[d] 20 *SMM*/GRS and *CGRO*/OSSE flares.

listed in Table 2 is difficult because the 0.847 MeV fluence is not well determined in many of them. Since we have found that fluxes of low-FIP emission lines correlate well with one another from flare to flare (Share & Murphy 1995), we chose to use the sum of the 0.847 (^{56}Fe), 1.238 (^{56}Fe), 1.369 (^{24}Mg), and 1.778 MeV (^{28}Si) lines as a monitor of the 0.847 MeV intensity. Calculated relative yields of these lines are reasonably constant for spectra harder than those with power indices of five (Murphy 1985). We demonstrate this good correlation in Figure 4 where we plot a comparison of the 0.847 MeV and low-FIP line fluences for the 20 flares listed in Table 2. The fluences are well correlated and the best-fit 0.847 MeV/(low FIP) ratio is 0.154 ± 0.022. This ratio does not differ significantly if we select only flares with accelerated-particle spectra with power-law indices consistent with 4. We note the low 0.847 MeV fluence for the 1982 December 7 flare (low FIP line fluence 43.5γ cm^{-2}); this flare exhibited an unusual spectrum suggestive of significant attenuation at energies below 1 MeV (Share & Murphy 1997b). We therefore use the scaled low-FIP line sum as a surrogate for the 0.847 MeV line in our comparison with the 0.937 and ~1.02 MeV lines in our studies below. Any reference to the "0.847 MeV" line reflects this utilization.

3.2.1. *Studies of the* 1.02 MeV *Line*

In Figure 5 we plot the measured ~1.02 MeV/"0.847 MeV" line ratios for the twenty flares versus the spectral indices of the accelerated particles inferred from measurements of the 6.13 MeV ^{16}O and 1.63 MeV ^{20}Ne lines. There are four panels in Figure 5 providing the measured ratios using fits with the appropriate ~1.02 MeV line profile provided in Mandzhavidze et al. (1997) for each model: (a) $\alpha/p = 0.1$, ^{3}He/^{4}He $= 0$; (b) $\alpha/p = 0.1$, ^{3}He/^{4}He $= 1$; (c) $\alpha/p = 0.5$, ^{3}He/^{4}He $= 0$; and (d) $\alpha/p = 0.5$, ^{3}He/^{4}He $= 1$. Note that the derived spectral indices differ for the two values of α/p. The dashed lines show the ratios calculated by Mandzhavidze et al. (1997).

Visual inspection indicates that the model fits the data best for cases (b) and (c). As mentioned above, valid quantitative comparisons of models with measured ratios using statistical weights cannot be done when the uncertainties

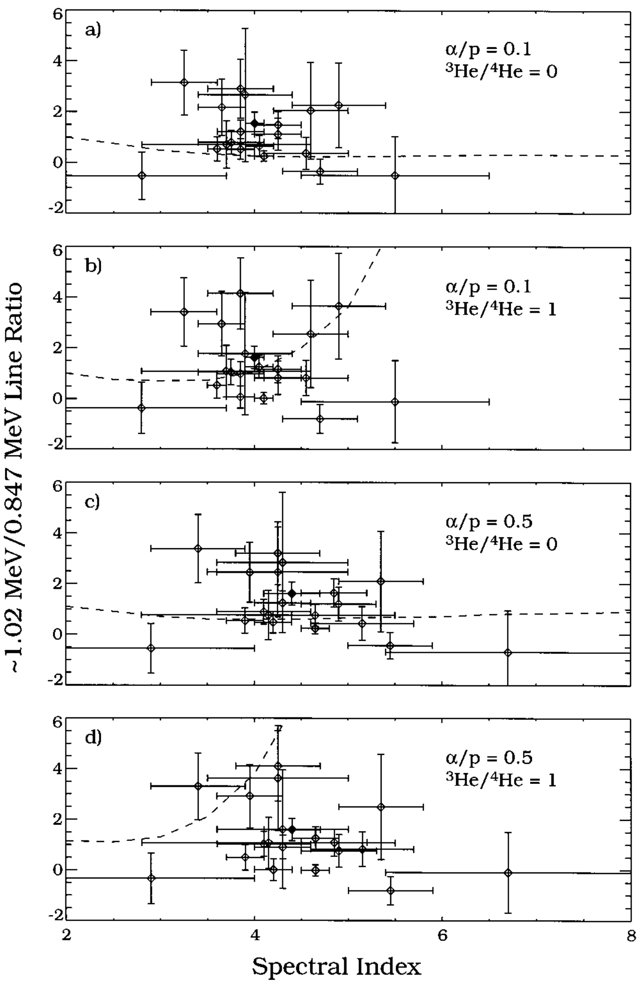

FIG. 5.—Measured ~1.02 MeV/"0.847 MeV" line ratios for 20 flares compared with spectral indices of the accelerated particles. The four panels show fitted ratios using the appropriate ~1.02 MeV line profile for (*a*) $\alpha/p = 0.1$, ^{3}He/^{4}He $= 0$; (*b*) $\alpha/p = 0.1$, ^{3}He/^{4}He $= 1$; (*c*) $\alpha/p = 0.5$, ^{3}He/^{4}He $= 0$; and (*d*) $\alpha/p = 0.5$, ^{3}He/^{4}He $= 1$. The filled symbol is the OSSE measurement. The calculated variation (Mandzhavidze et al. 1997) is shown by the dashed curve.

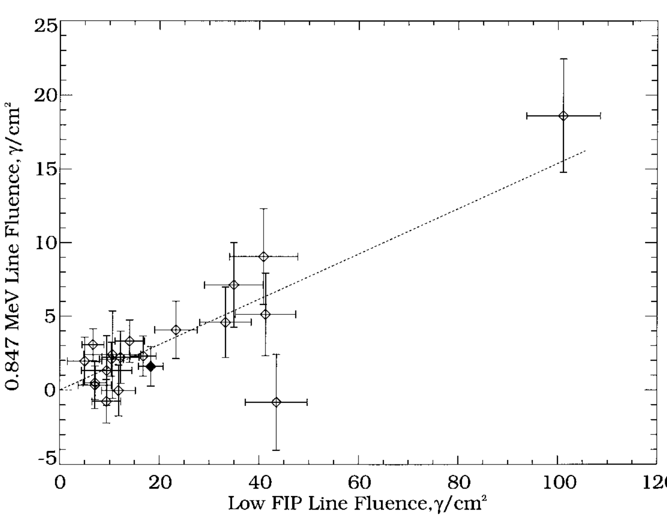

FIG. 4.—Comparison of 0.847 MeV line fluences with the sum of fluences from low-FIP lines at 0.847, 1.238, 1.369, and 1.778 MeV. Filled symbol is the OSSE observation of the 1991 June 4 flare. The dashed line shows the best-fitting slope, 0.154 ± 0.022.

are large enough to allow measured ratios close to 0. To quantify the comparison, we multiplied the measured "0.847 MeV" line fluence for each flare by the calculated ~1.02/0.847 MeV line ratio and compared the result with the measured ~1.02 MeV line fluence (a similar method was applied in § 2.1). This comparison is shown in Figure 6 for the four cases discussed above. Plotted are the differences between the observed and calculated ~1.02 MeV line fluences in units of the statistical uncertainty in σ. These uncertainties include the statistical errors in the "0.847 MeV" (low FIP) and ~1.02 MeV line fluences and in the calculated ~1.02/0.847 MeV ratios due to uncertainties in the spectral indices. Almost all of the observed ~1.02 MeV fluences are too high to be accounted for by the model for $\alpha/p = 0.1$ and ^{3}He/^{4}He $= 0$. The observations are, on average, a factor of 3.1 ± 0.5 higher than the calculations. For purposes of comparison we list the mean observed/calculated ratios of the ~1.02 MeV line for the four models in Table 3. The observations are, on average, in better agreement with the calculations for models (b) $\alpha/p = 0.1$, ^{3}He/^{4}He $= 1$ and (c) $\alpha/p = 0.5$, ^{3}He/^{4}He $= 0$, where the factors are 0.9 ± 0.2 and 1.3 ± 0.2, respectively. It is clear

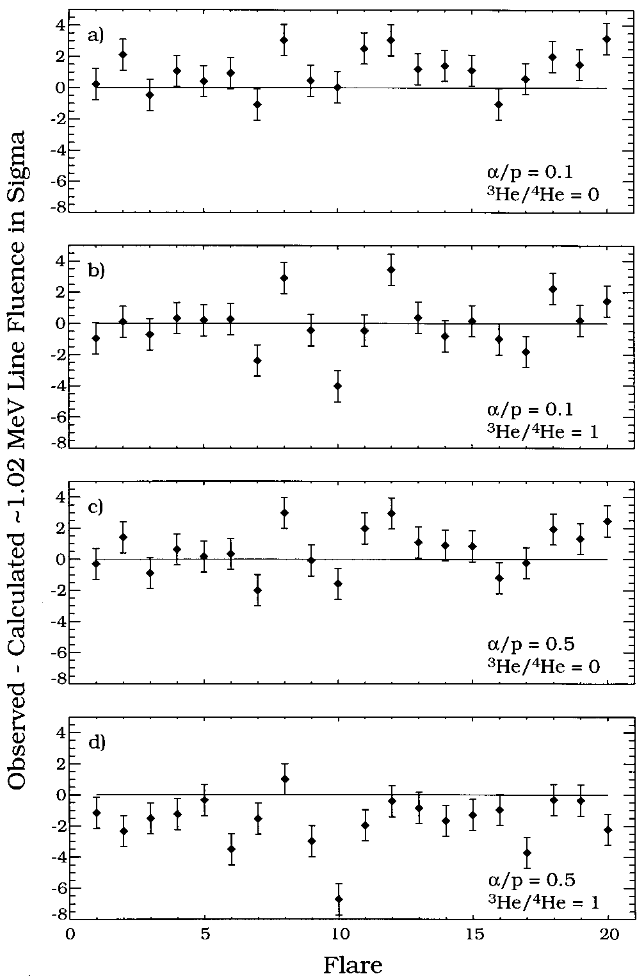

FIG. 6.—Differences between observed and calculated ~ 1.02 MeV line fluences for the 20 flares plotted in units of the statistical uncertainty in σ. (*a*) $\alpha/p = 0.1$, $^3He/^4He = 0$; (*b*) $\alpha/p = 0.1$, $^3He/^4He = 1$; (*c*) $\alpha/p = 0.5$, $^3He/^4He = 0$; and (*d*) $\alpha/p = 0.5$, $^3He/^4He = 1$.

that the data are inconsistent with the model for $\alpha/p = 0.5$, $^3He/^4He = 1$ because the observed fluences are, on average, only 0.15 ± 0.04 that of the calculations. From this comparison we are led to conclude that accelerated-particle compositions with either $\alpha/p = 0.1$ and $^3He/^4He = 1$ or $\alpha/p = 0.5$ and $^3He/^4He = 0$ are, on average, consistent with the data. This is also what Mandzhavidze et al. (1997) concluded from their study of the 1981 April 27 flare.

We can use the fits to the ~ 1.02 MeV line to set further constraints. If ^3He is a significant component of the accelerated particles, the line shape of the ~ 1.02 MeV feature should be significantly different and this change might be observable even with the moderate resolution of the NaI detectors used in this study (see Fig. 2). We investigated this possibility by creating a simulated count spectrum with a ~ 1.02 MeV line feature having the spectral shape expected from accelerated particles with $^3He/^4He = 1$ and then fitting this spectrum with the different models. We found that the fitted line strengths for models having $^3He/^4He = 1$ yielded intensities 45% higher than models having $^3He/^4He = 0$. When we fitted the individual spectra from the 20 flares using the spectral shape for $^3He/^4He = 1$, we found weak evidence for such an increase compared with fits using the spectral shape for $^3He/^4He = 0$; the fluences in the ~ 1.02 MeV line were increased on average by 19 ± 19% (for $\alpha/p = 0.1$) and by 8 ± 16% (for $\alpha/p = 0.5$). This suggests the presence of some ^3He in the accelerated-particle beam but not at a level comparable to that of ^4He. This is consistent with our fits to the summed spectra shown in Figure 2 that indicated an observed ~ 1.02 MeV line shape between those calculated for accelerated particles with $^3He/^4He = 0$ and 1 (see § 2.2).

3.2.2. *Studies of the* 0.937 MeV *Line*

The 0.937 MeV line provides another measure of the ^3He abundance in the accelerated particles. We compare the observed and calculated 0.937 MeV fluences for the four models. We obtained the calculated fluences by multiplying the "0.847 MeV" fluences by the 0.937 MeV/0.847 MeV ratio derived from the work of Mandzhavidze et al. (1997). In Figure 7 we plot the differences between the observed and calculated 0.937 MeV fluxes for the four models on a flare-by-flare basis. The solid data points are for flares with accelerated-particle spectral indices consistent with 4, the spectral index for which the 0.937 MeV/0.847 MeV ratios

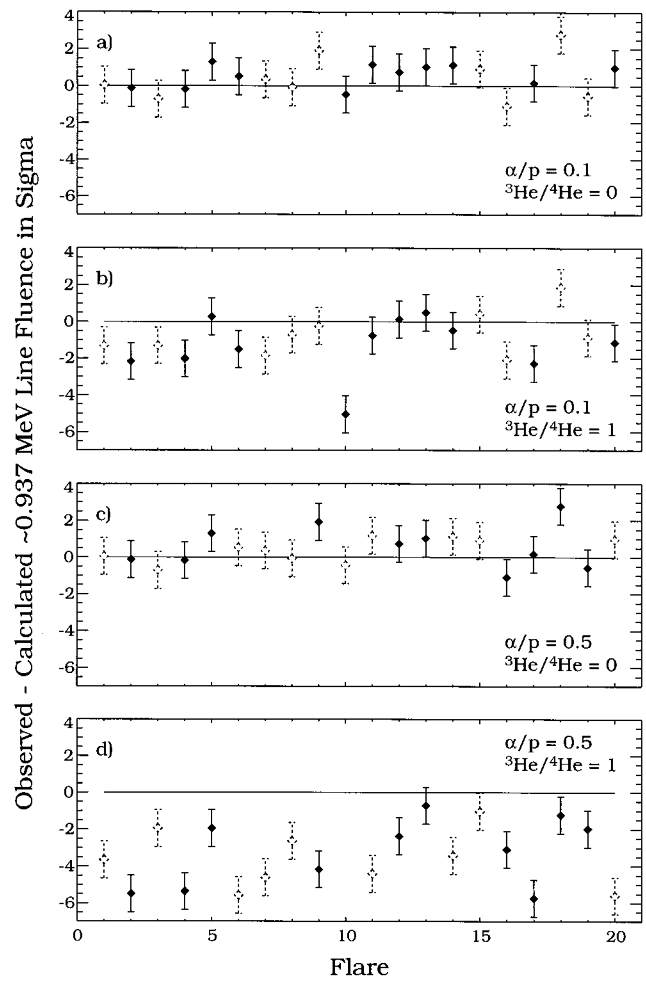

FIG. 7.—Differences between observed and calculated 0.937 MeV line fluences for the 20 flares plotted in units of the statistical uncertainty in σ. *Solid data points:* Flares with spectral indices consistent with a value of 4 for which the calculations were performed. *Dashed data points:* The remaining flares using the same calculations shown only for completeness. (*a*) $\alpha/p = 0.1$, $^3He/^4He = 0$; (*b*) $\alpha/p = 0.1$, $^3He/^4He = 1$; (*c*) $\alpha/p = 0.5$, $^3He/^4He = 0$; and (*d*) $\alpha/p = 0.5$, $^3He/^4He = 1$. In order to keep the plots uniform we have not plotted the difference ($-11.8\ \sigma$) for flare 10 in model d.

were calculated. For completeness we also plot the differences for the remaining flares (dashed data points) for reference. On average the observed 0.937 MeV fluences are consistent with but somewhat above the calculations for models a and c, where $^3He/^4He = 0$. In contrast, the observations on average are significantly below the predictions for $^3He/^4He = 1$. Because there is likely to be a spectral dependence in the 0.937 MeV/0.847 MeV ratio, we can only make a quantitative comparison for flares with spectral indices consistent with the value of 4 for which the calculations by Mandzhavidze et al. (1997) have been made. We used the χ^2 statistic discussed above. For this sample the observed and calculated (in parentheses) line ratios are (a) 0.32 ± 0.13 (0.1), (b) 0.39 ± 0.12 (1.1), (c) 0.46 ± 0.18 (0.1), (d) 0.5 ± 0.17 (4.9) for the four models. These results are also summarized in Table 3.

From our study of the $\sim$1.02 MeV line in § 3.2.1, only compositions with $\alpha/p = 0.1$ and $^3He/^4He = 1$ (model b) and $\alpha/p = 0.5$ and $^3He/^4He = 0$ (model c) provided adequate fits to the data. The yield of 0.937 MeV photons is much too low (by $\sim 6\ \sigma$) for particle compositions with $\alpha/p = 0.1$ and $^3He/^4He = 1$ (model b). In contrast, particle compositions with $\alpha/p = 0.5$ and $^3He/^4He = 0$ (model c) give better agreement with the observed 0.937 MeV flux (only $\sim 2\ \sigma$ high). These comparisons once again clearly rule out accelerated particles with $\alpha/p = 0.5$ and $^3He/^4He = 1$ (model d). In this 0.937 MeV study the $\alpha/p = 0.1$, $^3He/^4He = 0$ model a is also within 2 σ of agreeing with the observations, in contrast to its poor agreement in the $\sim$1.02 MeV study.

3.2.3. *Conclusions about Average* He *Abundances in Flares*

Considering all the different line studies we have discussed in this section (see Table 3) we can draw some general conclusions about the average ambient and accelerated He abundances in flares. The 0.339 MeV line studies indicate that the average ambient ^{4}He abundance in the flare interaction region is consistent with the accepted photospheric abundance, $\sim$8%. If this is true then the high α-^{4}He line fluxes observed in flares is likely to be caused by a high α/p ratio in flare-accelerated particles. Our independent analyses of the 0.937 and $\sim$1.02 MeV lines also suggest that an average accelerated-particle composition with a high α/p ratio ($\sim$0.5) is in best agreement with the data (model c: $\alpha/p = 0.5$ and $^3He/^4He = 0$). The fact that the measured 0.937 MeV and $\sim$1.02 MeV line fluences for this model are, on average, 1.5 to 2 σ above the calculations suggests that there is a significant amount of ^{3}He in the accelerated particles, but not at a level comparable to the concentration of ^{4}He.

In the next section we discuss any evidence for flare-to-flare variation in the He abundances.

3.2.4. *Studies of Flare-to-Flare Variations in* He *Abundances*

There is evidence for large flare-to-flare variations in the difference between the calculated and observed $\sim$1.02 MeV line fluxes plotted in Figure 6. The scatter is largest for models b and d. Since we have found that model c, $\alpha/p = 0.5$, $^3He/^4He = 0$, appears to fit the ensemble of flares best, we shall use it as the framework for studying flare-to-flare variations. The question we ask is whether there is evidence in individual flares for an unusually high ^{3}He abundance. Such evidence could take the form of a high $\sim$1.02 MeV line fluence coupled with a high 0.937 MeV fluence. Concentrating on Figure 6*c* we note that there are seven flares with observed $\sim$1.02 MeV emission more than 1 σ above what was predicted; these are flares numbered 2, 8, 11, 12, 18, 19, and 20. Of these we see from Figure 7*c* that flares numbered 11 and 18 showed some excess emission in the 0.937 MeV line as might occur if there were a higher ^{3}He concentration in the accelerated particles. For neither of these flares is there significant evidence for a $\sim$1.02 MeV line shape indicative of a high ^{3}He concentration as reflected in a higher flux when fitted by the $^3He/^4He = 1$ model (for flare 18 there was a 40% excess but the uncertainty was 70%; see Table 2). There is also no indication for a reduction in the 0.339 MeV fluences for these two flares, as might be expected if the high $\sim$1.02 MeV flux had not been due to a high accelerated α/p ratio. Mandzhavidze et al. (1997) also did not find a high ambient He/O ratio for these flares. Thus we find no compelling and consistent evidence for flare-to-flare variations in He abundances. More detailed studies of such variations are being performed by Ramaty & Mandzhavidze (1998), who calculate the spectral-index dependent 0.339 and 0.937 MeV line fluences for all the flares.

4. DISCUSSION

We have used moderate-resolution γ-ray spectrometers on *SMM* and *CGRO* to provide information on ambient and accelerated He in 20 flares. We find evidence for a weak line feature at 0.339 MeV from α-particle interactions on ^{56}Fe. By comparing the intensities of this line with the ^{7}Li and ^{7}Be lines produced by α-particle interactions on ^{4}He and using the calculations of Mandzhavidze et al. (1997), we estimated a flare-averaged ambient ^{4}He/H abundance ratio for about half of the flares. At the 68% level of confidence this ratio ranges from 0.04 to 0.11 and is thus consistent with the accepted photospheric value of $\sim$0.08. Owing to the weakness of the 0.339 MeV line, average ^{4}He/H abundance ratios up to 0.2 to 0.3 are still acceptable at the 5% level of confidence. If ambient ^{4}He in flare regions typically has a normal abundance, as is suggested here, then a relatively high concentration of accelerated α particles (α/proton $\sim$ 0.5) is necessary to explain the intense α-^{4}He fusion lines.

We have independently compared the intensities of lines at 0.847 MeV (from proton interactions on ^{56}Fe), at 0.937 MeV (from ^{3}He interactions on ^{16}O), and at $\sim$1.02 MeV (from both α-particle interactions on ^{56}Fe and ^{3}He interactions on ^{16}O). A high $\sim$1.02 MeV line intensity relative to the 0.847 MeV line, without a commensurate increase in the 0.937 MeV flux, would suggest an elevated accelerated α/proton (α/p) ratio in flares. Although we find evidence for some ^{3}He in the accelerated particles from the elevated level in the 0.937 MeV line and the shape of the $\sim$1.02 MeV line, its concentration is on average too low to fully account for the strong $\sim$1.02 MeV line feature. This once again suggests that a high concentration of accelerated α particles ($\alpha/p \sim 0.5$) typically occurs in flares.

More comprehensive studies (e.g., Ramaty & Mandzhavidze 1998) using the data presented here and calculations of spectral dependent line yields for varying accelerated α/p ratios will provide a better understanding of the He composition in flares. These studies will also allow a complete investigation of flare-to-flare variations, although the weakness of the lines in individual events may prevent any firm conclusions on variability to be drawn.

It is a pleasant surprise that the moderate-resolution spectrometers on *SMM* and *CGRO* have been able to even provide this much information. Additional observations of nuclear line flares with the *CGRO*/OSSE instrument are planned for cycle 23. Improved spectral observations of flares with NASA's High-Energy Solar Spectroscopic Imager (HESSI) high-resolution γ-ray spectrometer can provide more definitive measurements, especially using the narrow line at 0.339 MeV.

This work has been supported by NASA DPR W-18995 and S-57769F. These unexpected spectroscopic studies are a tribute to our colleagues who designed, built, and operated the excellent *SMM* and *CGRO* spectrometers. We wish to thank Ed Chupp, Dave Forrest, Claus Reppin, Jim Ryan, and Tom Vestrand for their work on *SMM* and Eric Grove, Neil Johnson, Bob Kinzer, Dick Kroeger, Jim Kurfess, and Mark Strickman for their efforts on *CGRO*.

REFERENCES

Hua, X.-M., & Lingenfelter, R. E. 1987, ApJ, 319, 555
Johnson, W. N., et al. 1993, ApJS, 86, 693
Mandzhavidze, N., Ramaty, R., & Kozlovsky, B. 1997, ApJ, 489, L99
Murphy, R. J. 1985, Ph.D. thesis, Univ. Maryland
Murphy, R. J., Kozlovsky, B., & Ramaty, R. 1988, ApJ, 331, 1029
Murphy, R. J., Share, G. H., Letaw, J. R., & Forrest, D. J. 1990, ApJ, 358, 298
Murphy, R. J., et al. 1997, ApJ, 490, 883
Ramaty, R., & Lingenfelter, R. E. 1995, in Proc. STScI Symp., ed. R. Williams & M. Livio (Cambridge: Cambridge Univ. Press), 180
Ramaty, R., & Mandzhavidze, N. 1998, in Eos Suppl. AGU Spring Meeting (Washington, DC: AGU), S279
Share, G. H., & Murphy, R. J. 1995, ApJ, 452, 933
———. 1997a, ApJ, 484, L165
———. 1997b, ApJ, 485, 409
Share, G. H., Murphy, R. J., & Skibo, J. G. 1996, in AIP Conf. Proc. 374, High-Energy Solar Physics, ed. R. Ramaty & N. Mandzhavidze (New York: AIP), 162